Atomic-Scale Structure of Single-Layer MoS_2 Nanoclusters

S. Helveg,[1] J. V. Lauritsen,[1] E. Lægsgaard,[1] I. Stensgaard,[1] J. K. Nørskov,[2] B. S. Clausen,[3]
H. Topsøe,[3] and F. Besenbacher[1,*]
[1]*CAMP and Institute of Physics and Astronomy, University of Aarhus, DK-8000 Aarhus C, Denmark*
[2]*CAMP and Physics Department, Technical University of Denmark, DK-2800 Lyngby, Denmark*
[3]*Haldor Topsøe Research Laboratories, Nymøllevej 55, DK-2800 Lyngby, Denmark*

(Received 11 October 1999)

We have studied using scanning tunneling microscopy (STM) the atomic-scale realm of molybdenum disulfide (MoS_2) nanoclusters, which are of interest as a model system in hydrodesulfurization catalysis. The STM gives the first real space images of the shape and edge structure of single-layer MoS_2 nanoparticles synthesized on Au(111), and establishes a new picture of the active edge sites of the nanoclusters. The results demonstrate a way to get detailed atomic-scale information on catalysts in general.

PACS numbers: 82.65.Jv, 61.16.Ch, 61.46.+w, 77.84.Bw

With the advent of the scanning tunneling microscope (STM) scientists now have a tool to directly image nanoscale structures on surfaces. This has opened up the field of nanotechnology where the aim is to make nanostructures with interesting functional properties. Up to now, the interest has been focused mainly on metal and semiconductor nanostructures [1]. In this Letter, we show how to synthesize and characterize transition metal sulfide nanoclusters. These are of interest as lubricants [2], as models of the active part of some enzymes [3], and as hydrodesulfurization (HDS) catalysts [4,5], which currently receive special attention due to the worldwide demand for cleaner transport fuels. Here we focus on MoS_2 nanostructures, as a model system of an HDS catalyst. MoS_2 nanocrystals, single layer in height and ~30 Å wide, are synthesized using the Au(111) surface as a template.

Atom-resolved STM images reveal that the small clusters exhibit triangular morphology, contrary to the expectation from bulk MoS_2. The catalytically important MoS_2 edges are found to be reconstructed relative to the perfect MoS_2 lattice. The first direct images are presented of the catalytically active sites in the form of S vacancies at the edges of MoS_2, created by *in situ* treatment of the nanoclusters to atomic hydrogen.

The experiments were performed in a standard ultrahigh vacuum (UHV) chamber equipped with a homebuilt, high-resolution STM capable of resolving the individual atoms of close-packed surfaces and clusters on a routine basis [6]. The Au(111) substrate surface was sputter-cleaned by 1.5 keV Ar ion bombardment followed by annealing at 900 K. The Au(111) surface was chosen as a model substrate, since gold is noble and chemically inert [7], and since the characteristic herringbone reconstruction, which exists for this surface [8], is ideal for providing nucleation sites for epitaxial growth of highly dispersed metal islands [9]. Indeed, when molybdenum was deposited on the Au(111) surface using an e-beam evaporator, a self-assembled regular array of one or two layer high Mo islands is formed [Fig. 1(a)] extending over a mesoscopic length scale. The average lateral spacings between the ~30 Å wide Mo clusters are 73 and 140 Å, corresponding to the lattice parameters of the unit cell of the reconstructed Au(111) superlattice. Thus, the Au(111) surface acts as a template to disperse the Mo into small islands, which facilitates the subsequent sulfidation into MoS_2 nanocrystals.

We have explored a number of different sulfidation procedures. In the results discussed below, the Mo is evaporated in an H_2S atmosphere of 1×10^{-6} mbar at 400 K, and subsequently, the crystal is annealed at 673 K for 15 min while maintaining the H_2S background pressure. In this case, the majority of the Mo islands are transformed into crystalline MoS_2 nanoclusters. It is noteworthy that with respect to morphology, the majority of the nanoclusters are seen to be triangular in shape [Fig. 1(b)] with a side length of ~30 Å. The orientations of the triangles reflect the sixfold symmetry of the substrate. As will be discussed below, these clusters are interpreted as one layer thick MoS_2 nanocrystallites lying flat on the surface with the basal (0001) plane of the MoS_2 particles being oriented parallel to the Au(111) substrate.

Figure 2 depicts an atomically resolved STM image of one of the triangular clusters from Fig. 1(b). The protrusions are arranged with hexagonal symmetry with an average interatomic spacing of 3.15 ± 0.05 Å. This is exactly the interatomic spacing of S atoms in the (0001) basal plane of MoS_2, which is a layered compound, consisting of stacks of S-Mo-S sandwiches held together by van der Waals interactions. Each sandwich is composed of two hexagonal planes of S atoms and an intermediate hexagonal plane of Mo atoms, trigonal prismatically coordinated to the S atoms. Before we proceed, it is important to point out that low bias, constant current STM images reflect the local density of states at the Fermi level projected to the position of the tip apex [10]. In general, the images thus reflect a convolution of the geometric and electronic structure of the surface. However, STM calculations on layered MoS_2 slabs show that for typical tunneling distances, only the S atoms in the topmost layer are imaged [11]. Since our STM images did not change by varying the tunnel

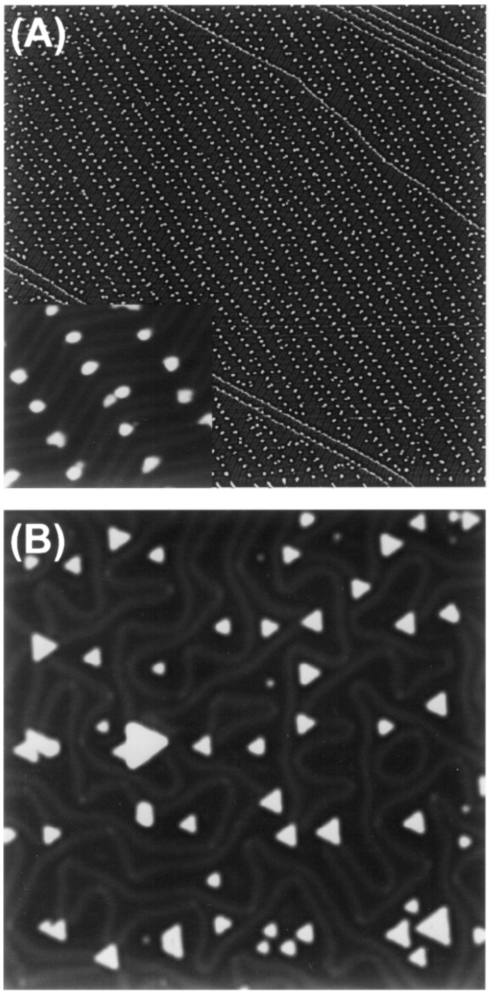

FIG. 1. (a) An STM image (4035 Å × 4090 Å) of Mo deposited onto Au(111) at 307 K under UHV conditions. The inset is a close-up (397 Å × 354 Å) showing the herringbone reconstruction of the Au(111) [8]. The regular array of elbows on the dislocation lines acts as nucleation sites for the Mo [9]. (b) An STM image (744 Å × 721 Å) of the sulfided Mo clusters on Au(111). Mo is deposited in 1.0×10^{-6} mbar H_2S while the gold substrate was cooling down from 420 K to 357 K. Subsequently, the surface is annealed to 673 K in the H_2S atmosphere.

current, we interpret the triangular-shaped islands in the STM images to be MoS_2 nanocrystallites with their (0001) basal plane being oriented parallel to the Au(111) substrate surface and with the protrusions reflecting the hexagonally arranged S atoms in the topmost S layer. In 2H-MoS_2, which is the common form found in nature, the unit cell contains two S-Mo-S layers. Since the triangular-shaped islands (Fig. 2) have an apparent height of only 2.0 ± 0.3 Å, we conclude that the MoS_2 nanoclusters are present as single layers on the Au surface. Thus, only one of the two building blocks of the unit cell is present.

With respect to the morphology of the MoS_2 nanoclusters, the STM images directly reveal that the clusters are of triangular shape under the present sulfiding conditions. In principle, the morphology of a MoS_2 slab should be determined by two types of edge terminations, a $(\bar{1}010)$ S-edge and a $(10\bar{1}0)$ Mo-edge. In Fig. 3(a), the two edges are illustrated for a hypothetical hexagonal MoS_2 cluster, where the edges are simple terminations of the bulk MoS_2 structure. In the 2H bulk stacking sequence, alternate MoS_2 layers will expose Mo and S edges, respectively. One would thus expect that bulk crystals or multilayer clusters preferentially grow in a hexagonal morphology, since the difference in edge energies tends to cancel. The observed triangular shape (Fig. 1) may therefore be a unique feature of the single-layer MoS_2 clusters, and the triangular shape implies that one of the edge terminations is considerably more stable. Based on a simple Wulff type construction argument [12] (see inset of Fig. 2), we can indeed conclude that the ratio of the specific surface free energy of the Mo edge to the S edge, or vice versa, is at least a factor of 2 under the present sulfiding conditions. The fact that the single-layer MoS_2 nanoclusters have a morphology different from that for bulk MoS_2 nanoclusters might be interesting, since previous studies have shown that single and multilayer MoS_2 slabs have different catalytical properties [5].

To resolve which of the two edge structures is the more stable, we zoom in on the edge structure of the triangles. If we assume that also the edge protrusions are associated with S atoms, we can, from the grid superimposed in Fig. 2, conclude that the S atoms at the edges are out of registry with the S atoms in the hexagonal lattice of the basal plane. In fact, the S atoms are observed to be shifted by half a lattice constant along the edge.

The question of which edge termination is the more stable is complicated by the fact that under the present sulfiding conditions, the edges may not be simple terminations of the stoichiometric MoS_2 as depicted in Fig. 3(a). Recent density functional theory (DFT) calculations [13,14] have shown for the Mo terminated edge structures typically either one [Fig. 3(d)] or two [Fig. 3(c)] S atoms per Mo edge atoms are present. In both cases, the Mo atoms are coordinated to six S atoms, i.e., saturated with S as for the Mo atoms in bulk MoS_2, and thus the two structures have almost the same stability. However, the DFT calculations [13] show that only the structure with one S atom per Mo edge atom [Fig. 3(d)] results in S atoms at the edge, which are shifted by half a lattice constant relative to the S atoms in the basal plane, as in the STM images. For the S terminated edges none of the calculated structures appear to be reconstructed and thus consistent with the STM findings [13]. We therefore conclude that the model illustrated in Fig. 3(e) is the structure observed.

Previous studies have shown that the MoS_2 basal plane is fairly inactive [15], and that the HDS reactivity occurs preferentially at the MoS_2 edges [5,15,16]. The nanostructures shown in Fig. 1(b) are formed under sulfiding conditions, where all Mo atoms, even at the edges, appear to have a S coordination number of six. However, it is generally believed that such structures are not the most active ones in HDS catalysis, i.e., undercoordinated Mo

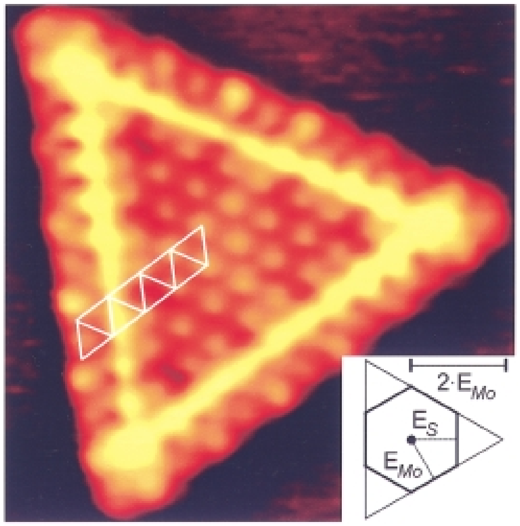

FIG. 2 (color). An atom-resolved STM image (41 Å × 42 Å, $I_t = 1.28$ nA and $V_t = 5.2$ mV) of a MoS_2 nanocluster. The grid shows the registry of the edge atoms relative to those in the basal plane of the MoS_2 triangle. The inset shows a Wulff construction of the MoS_2 crystal. E_{Mo} and E_S denote the free energy for the Mo and S edges, respectively.

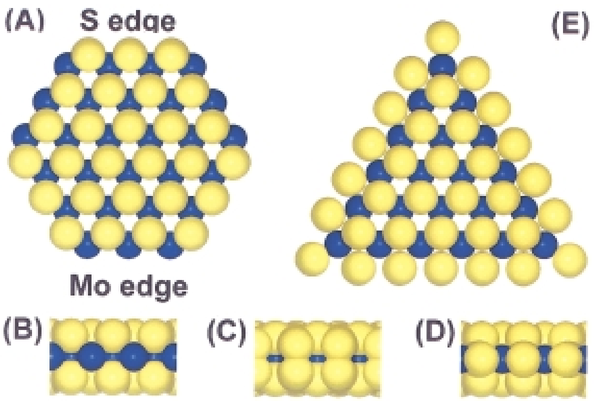

FIG. 3 (color). (a) A ball-model (top view) of a bulk truncated MoS_2 hexagon with Mo and S edges being exposed. The Mo (blue) atoms at the Mo edges are coordinated to only four S atoms (yellow), whereas the Mo atoms in the bulk are coordinated to six S atoms. (b)–(d) Side view of Mo edges. (b) The naked Mo edge in (a). (c) The Mo edges are terminated with S atoms resulting in S dimers at the edges; i.e., we have 2 S per Mo atom at the edges. In (d) there is only one S atom per Mo atom at the edges. In this case, the S edge is reconstructed with respect to the S dimer model in (c). The S atoms move vertically to the Mo plane and shift laterally with half a lattice constant. (e) A top view of (d). Models (d) and (e) depict the triangular structure observed in the STM images with the S edge atoms being out of registry with the S atoms in the basal plane of MoS_2.

atoms must be formed by sulfur removal before hydrodesulfurization can take place [5,17]. We have performed the first preliminary experiments to create such S vacancies and thus produce the active sites for the HDS catalytic reaction by exposing the MoS_2 nanoclusters to atomic hydrogen produced by dissociating H_2 on a hot W filament. Figure 4 shows an STM image of the resulting structures, which clearly demonstrates that hydrogen has stripped off a few of the S atoms at the edges forming S vacancies. It is thus likely that we are directly imaging, on an atomic scale, the catalytically active sites for the HDS reaction. The energy involved in creating a vacancy is calculated within the DFT scheme to be 0.6 eV [13,18]. By exposing the sulfided structure to low doses of very reactive H atoms, this energy barrier is surmounted. Under ordinary HDS conditions the high pressures of H_2 and higher temperatures ensure a reasonable population of the active sites.

In the past, it has been speculated that the MoS_2 clusters could exist in different shapes (hexagonal, truncated hexagonal, rhombohedral, etc.), but direct experimental evidence of such structures has been lacking [5]. Similarly, the lack of suitable experimental techniques to reveal the atomic-scale structure of the edges has led researchers to assume that the Mo and S atoms at the edges are located at the bulk truncated atomic positions. The present STM results thus provide new insight into both the morphology (shape) and the edge structures of MoS_2 nanoclusters. We have shown that it is possible to synthesize MoS_2 nanostructures and to resolve their structure at the atomic scale. We have presented the first direct real space STM images of the shape and edge structure of single-layer high MoS_2

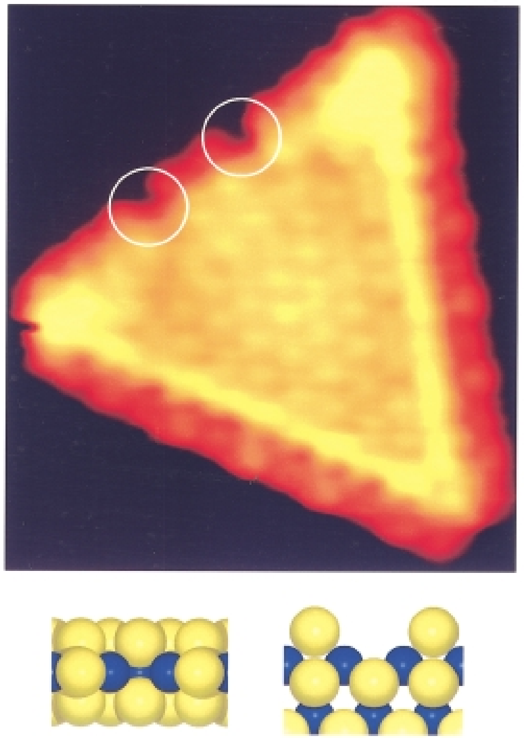

FIG. 4 (color). An atom-resolved STM image ($I_t = 1.12$ nA and $V_t = -8.5$ mV) of a MoS_2 nanocluster exposed to atomic hydrogen at 600 K which resulted in the formation of S vacancies at the edges indicated by the white circles. A model (a side and a top view) is shown in which a S vacancy has been formed in the structure (d) in Fig. 3.

nanoparticles, and have experimentally established a new picture of active sites. The approach presented here should be applicable to inorganic clusters deposited on conducting substrates in general. Such detailed atomic-scale information may aid in the development of, e.g., better catalysts.

We acknowledge stimulating discussions with L. Pleth Nielsen and L. S. Byskov, and financial support from the VELUX and the Knud Højgaard Foundations. The Center for Atomic-scale Materials Physics (CAMP) is sponsored by The Danish National Research Foundation. S. H. acknowledges support from the Danish Research Academy and the Interdisciplinary Center for Catalysis (ICAT).

---

*Corresponding author.
Email address: fbe@ifa.au.dk

[1] S. Völkening *et al.*, Phys. Rev. Lett. **83**, 2672 (1999); M. Hildebrand, A. S. Mikhailov, and G. Ertl, Phys. Rev. Lett. **81**, 2602 (1998); B. Müller *et al.*, Phys. Rev. Lett. **80**, 2642 (1998); V. P. Zhdanov and B. Kasemo, Phys. Rev. Lett. **81**, 2482 (1998); M. Böhringer *et al.*, Phys. Rev. Lett. **83**, 324 (1999).

[2] T. Spalvins, J. Vac. Sci. Technol. A **5**, 212 (1987).

[3] E. I. Stiefel, in *Transition Metal Sulfur Chemistry, Biological and Industrial Significance,* edited by E. I. Stiefel and K. Matsumoto, ACS Symposium Series Vol. 653 (American Chemical Society, Washington, DC, 1996).

[4] R. Prins, in *Handbook of Heterogenous Catalysis,* edited by G. Ertl, H. Knözinger, and J. Weitlamp (VHC Verlagsgesellschaft mbH, Weinheim, 1997); J. C. Muijsers, T. Weber, R. M. van Hardeveld, H. W. Zandbergen, and J. W. Niemantsverdriet, J. Catal. **157**, 698 (1995); E. Hensen and R. A. van Santen, Cattech **3**, 86 (1998).

[5] H. Topsøe, B. S. Clausen, and F. E. Massoth, *Hydrotreating Catalysis, Science and Technology* (Springer-Verlag, Berlin, 1996).

[6] E. Lægsgaard *et al.*, J. Microsc. **152**, 663 (1988); F. Besenbacher, Rep. Prog. Phys. **59**, 1737 (1996).

[7] B. Hammer and J. K. Nørskov, Phys. Rev. Lett. **76**, 2141 (1996); Nature (London) **376**, 238 (1995).

[8] J. V. Barth, H. Brune, G. Ertl, and R. J. Behm, Phys. Rev. B **42**, 9307 (1990).

[9] D. D. Chambliss, R. J. Wilson, and S. Chiang, Phys. Rev. Lett. **66**, 1721 (1991).

[10] J. Tersoff and D. R. Hamann, Phys. Rev. B **31**, 805 (1985).

[11] A. Altibelli, C. Joachim, and P. Sautet, Surf. Sci. **367**, 209 (1996); K. Kobayashi and J. Yamauchi, Phys. Rev. B **51**, 17 085 (1995).

[12] G. Wulff, Z. Kristallogr. **34**, 449 (1901); T. Michely, M. Hohage, M. Bott, and G. Comsa, Phys. Rev. Lett. **70**, 3943 (1993).

[13] L. S. Byskov, J. K. Nørskov, B. S. Clausen, and H. Topsøe, Catal. Lett. **47**, 177 (1997); J. Catal. **187**, 109 (1999).

[14] P. Raybaud, J. Hafner, G. Kresse, and H. Toulhoat, Surf. Sci. **407**, 237 (1998).

[15] M. Salmeron *et al.*, Chem. Phys. Lett. **90**, 105 (1982); J. G. Kushmerick and P. S. Weiss, J. Phys. Chem. **102**, 10 094 (1998).

[16] S. J. Tauster, T. A. Pecoraco, and R. R. Chianelli, J. Catal. **63**, 515 (1980); P. Raybaud, J. Hafner, G. Kresse, and H. Toulhoat, Phys. Rev. Lett. **80**, 1481 (1998).

[17] J. K. Nørskov, B. S. Clausen, and H. Topsøe, Catal. Lett. **13**, 1 (1992).

[18] This is the energy for the reaction $^{*}S + H_2 \rightarrow {}^{*} + H_2S$, where * denotes an S vacancy, or an active site.